

# CONTROL STRATEGY FOR THE DOUBLE-BOOST CONVERTER IN CONTINUOUS CONDUCTION MODE APPLIED TO POWER FACTOR CORRECTION

Alexandre S. Martins, Enio V. Kassick and Ivo Barbi

Federal University of Santa Catarina  
Dept. of Electrical Engineering  
Power Electronics Institute

P.O. BOX 5119 - 88040-970 - Florianópolis - SC - Brazil  
Phone : 55-48-231.9204 - Fax : 55-48-231.9770 - e-mail : kassick@inep.ufsc.br

**Abstract** - This paper deals with the control strategy for the Double Boost Converter in Power Factor Correction (PFC) application, working in Continuous Conduction Mode (CCM). This converter is based on the classic Boost Converter split into two parallel modules of power processing; each one of this modules process half of nominal power of the converter. Technical literature concerning this converter do not deeply analyze some very important control aspects and it seems that it is still lacking a general control strategy for such converter. This subject will be developed in the present paper. This is done by converter modeling based upon the PWM switch model. The model obtained, verified by simulations, points to a multivariable control system, since the converter output voltages and the control variables (duty cycle of the two active switches) are strongly coupled. It is applied the dynamic uncoupling technique in order to overcome this undesirable characteristic and to design the voltage and current compensation loops. Each module of power processing has a current mode controlled PFC circuit with a current-regulation inner loop and a voltage-regulation outer loop and the dynamic uncoupling is performed over the former. Numerical simulation results of the behavior of the Double-Boost Converter for Power Factor Correction application are presented.

## 1 - INTRODUCTION

The Boost Converter is largely applied for power factor correction (PFC) due to its intrinsic characteristics. The basic scheme for this kind of application is shown in figure 1.

Even if this converter presents a good performance for PFC general applications, for high power associated to a wide input voltage range variation (110 V<sub>RMS</sub> and 220 V<sub>RMS</sub> input voltage, for instance), the converter performance is poor, and a lot of drawbacks arise.

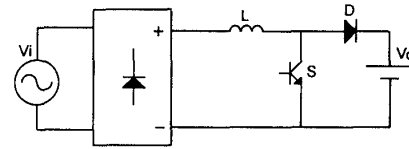


Figure 1: Boost Converter for power factor correction (PFC) applications.

In order to overcome these drawbacks the so-called Double-Boost Converter may be employed [1]-[2]. This converter shown in figure 2, may be seen as a Boost converter split in two modules, where each module processes half of the total output power.

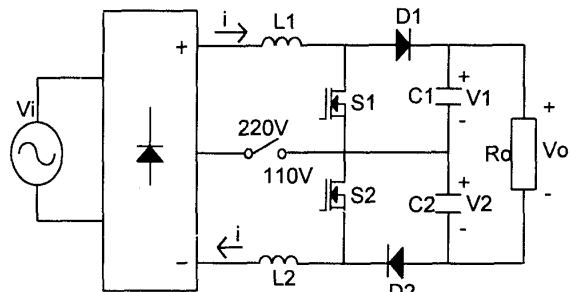


Figure 2: Double-Boost Converter.

Ideally, one can expect that, if the same drive signal is employed to command the two active switches  $S_1$  and  $S_2$ , they will present exactly the same conduction and commutation times, implying that the output voltage  $V_o$  will be equally distributed over the two output capacitors  $C_1$  and  $C_2$ .

In fact, laboratory results indicate that, in practice and for 220 V<sub>RMS</sub> line voltage, small differences between the conduction and commutation times of the two active switches, even if these differences are infinitesimal, provoke, as time goes by, a bascule or swing effect over the capacitors voltage, in such a way that the total output voltage remains over one of them, while voltage become zero over the other one.

This behavior can be easily understood with the aid of figures 3 (a) and (b). In the first one, switch  $S_2$  remains “on” while switch  $S_1$  is already “off” (remember that even if this difference is infinitesimal, this phenomenon will be repeated for each switching period, causing an integrative effect).

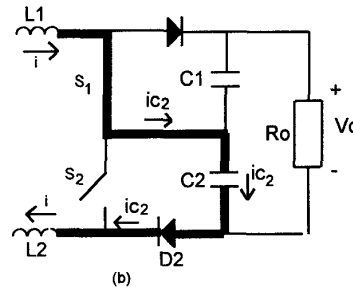
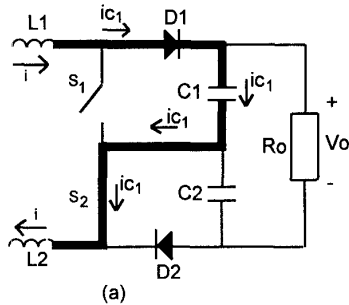


Figure 3: Physical interpretation of the bascule or swing effect of the capacitors voltage.

It is clear that for such situations the total output power will be processed just by one module of the Double-Boost Converter, and the main capability of sharing power is lost.

It seems necessary to implement an efficient control strategy to provide the equalization of the capacitor voltages. References do not analyze deeply this subject; so, the principal aim of the present paper is to propose a control strategy and to do that, a modeling approach will be employed in order to well understand the verified behavior and also to establish the required control action.

## 2 - DOUBLE-BOOST CONVERTER MODELING

The design of the controller requires the knowledge of both the boost inductor current and the output capacitors voltages transfer functions with respect to the control variables  $\hat{d}1(s)$  and  $\hat{d}2(s)$ , namely the duty cycles of main switches  $S_1$  and  $S_2$ , respectively.

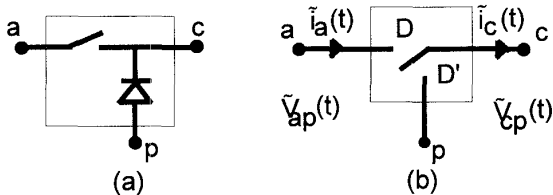


Figure 4: (a) active and passive switches, (b) single three-terminal switching device.

To establish these transfer functions one can employ the PWM Switch Model [3], for Continuous Conduction Mode (CCM). Figure 4 (a) and (b) shows the active and passive switches and

It is easy to show that in this case, capacitor  $C_1$  will be charged with a slightly greater amount of charge in each switching period, causing a progressive increase of its voltage. Figure 3(b) shows the same effect concerning now switch  $S_1$  and capacitor  $C_2$ .

the corresponding PWM switch model, lumped as a single three-terminal switching device, where:

a  $\Rightarrow$  active terminal

p  $\Rightarrow$  passive terminal

c  $\Rightarrow$  common terminal

$\tilde{i}_a(t) \Rightarrow$  instantaneous active terminal current

$\tilde{i}_c(t) \Rightarrow$  instantaneous common terminal current

$\tilde{V}_{ap}(t) \Rightarrow$  instantaneous voltage across port ap

$\tilde{V}_{cp}(t) \Rightarrow$  instantaneous voltage across port cp

D  $\Rightarrow$  on-time duty cycle

$D' = 1 - D$

Notice that expressions (1) and (2) present the invariant relations between the average terminal voltages and currents of the PWM switch, where  $d$  is the average value of on-time duty cycle.

$$i_a = d \cdot i_c \quad (1)$$

$$v_{cp} = d \cdot v_{ap} \quad (2)$$

In the same way Figure 5 and expressions (3) to (6) represent the small-signal model of the PWM switch.

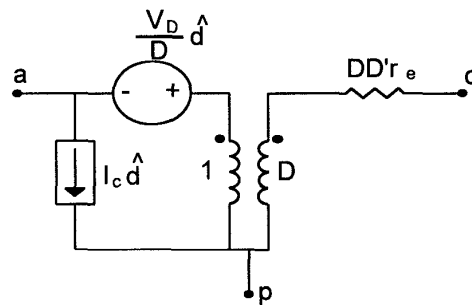


Figure 5: Small-signal model of PWM switch.

$$\hat{i}_a = D\hat{i}_c + I_c\hat{d} \quad (3)$$

$$\hat{v}_{cp} = D(\hat{v}_{ap} + I_c r_e \hat{d} - \hat{i}_c r_c D') + \hat{d}(V_{ap} - I_c r_c D') \quad (4)$$

$$\hat{v}_{ap} = \frac{\hat{v}_{cp}}{D} + \hat{i}_c r_c D' - \frac{V_D}{D} \hat{d} \quad (5)$$

where:

$$V_D = V_{ap} + I_c (D - D') r_e \quad (6)$$

The symbol  $\hat{\phantom{x}}$  denotes the perturbed average value of the concerned voltage, current or duty cycle.

It is important to remark that  $V_{ap}$ ,  $I_c$  and  $D$  represent the DC operating point of the PWM switch, which can be obtained starting from the circuit presented in Figure 5, when the perturbed average values becomes zero and the voltage and current sources becomes a short circuit and an open circuit respectively.

As can be observed in Figure 2, switch  $S_1$  and diode  $D_1$  constitute one PWM switch and switch  $S_2$  and diode  $D_2$  constitute another one. So, replacing the real switches and diodes by the small-signal model of the PWM switch as shown in Figure 5, one can arrive to the circuit presented in Figure 6, where the series resistances of the inductors and capacitors were added. Notice also that, in order to establish the transfer functions related to the inductor current and to the capacitors output voltages, the input voltage source (in this case, the rectifier output voltage) is shorted to ground.

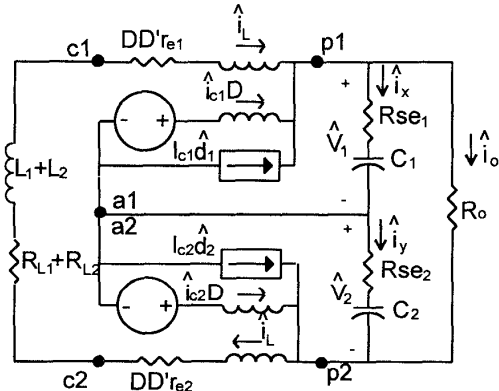


Figure 6: Double-Boost Converter equivalent circuit for small-signal analysis.

$$B_1 = B_2 = \frac{C_1 C_2 \left\{ (R_o + R_{se1} + R_{se2}) [R_{L1} + R_{L2} + (r_{e1} + r_{e2}) DD'] + (R_{se1} + R_{se2}) D'^2 R_o \right\} + (L_1 + L_2) (C_1 + C_2)}{C_1 C_2 (L_1 + L_2) (R_o + R_{se1} + R_{se2})} \quad (16)$$

## 2.1 - DOUBLE-BOOST INDUCTOR CURRENT TRANSFER FUNCTION

Expressions (7) to (9) presents, in the Laplace domain, the Double-Boost inductor current  $\hat{i}(s)$  as a function of switches  $S_1$  and  $S_2$  duty cycles  $\hat{d}_1(s)$  and  $\hat{d}_2(s)$ . The values of  $K_1$ ,  $K_2$ ,  $A_1$ ,  $A_2$ ,  $B_1$ ,  $B_2$ ,  $C_1$  and  $C_2$  are defined by converter parameters, as presented by expressions (10) to (16).

$$\hat{i}(s) = G_1(s)\hat{d}_1 + G_2(s)\hat{d}_2 \quad (7)$$

where

$$G_1(s) = K_1 \frac{s + A_1}{s^2 + sB_1 + C_1} \quad (8)$$

$$G_2(s) = K_2 \frac{s + A_2}{s^2 + sB_2 + C_2} \quad (9)$$

and

$$K_1 = \frac{(R_o + R_{se1} + R_{se2}) \left( V_1 + \frac{V_o}{R_o D'} (D - D') r_{e1} \right) + V_o R_{se1}}{(L_1 + L_2) (R_o + R_{se1} + R_{se2})} \quad (10)$$

$$K_2 = \frac{(R_o + R_{se1} + R_{se2}) \left( V_2 + \frac{V_o}{R_o D'} (D - D') r_{e2} \right) + V_o R_{se2}}{(L_1 + L_2) (R_o + R_{se1} + R_{se2})} \quad (11)$$

$$C_1 = C_2 = \frac{(R_{L1} + R_{L2}) + (r_{e1} + r_{e2}) DD' + D'^2 R_o}{(L_1 + L_2) (R_o + R_{se1} + R_{se2})} \quad (12)$$

$$r_{e1} = r_{e2} = \frac{(R_{se1} + R_{se2}) R_o}{R_{se1} + R_{se2} + R_o} \quad (13)$$

$$A_1 = \frac{(C_1 + C_2) \left( V_1 + \frac{V_o}{R_o D'} (D - D') r_{e1} \right) + V_o C_2}{C_1 C_2 \left( (R_o + R_{se1} + R_{se2}) \left( V_1 + \frac{V_o}{R_o D'} (D - D') r_{e1} \right) + V_o R_{se1} \right)} \quad (14)$$

$$A_2 = \frac{(C_1 + C_2) \left( V_2 + \frac{V_o}{R_o D'} (D - D') r_{e2} \right) + V_o C_1}{C_1 C_2 \left( (R_o + R_{se1} + R_{se2}) \left( V_2 + \frac{V_o}{R_o D'} (D - D') r_{e2} \right) + V_o R_{se2} \right)} \quad (15)$$

## 2.2 - OUTPUT CAPACITOR VOLTAGES TRANSFER FUNCTIONS

Expression (17) presents the output capacitor voltages transfer functions, in the Laplace domain, as functions of switches  $S_1$  and  $S_2$  duty cycles  $\hat{d}_1(s)$  and  $\hat{d}_2(s)$ . It is easy to remark that voltages  $\hat{V}_1(s)$  and  $\hat{V}_2(s)$  are coupled with  $\hat{d}_1(s)$  and  $\hat{d}_2(s)$  by means of a transference matrix.

$$\begin{bmatrix} \hat{V}_1(s) \\ \hat{V}_2(s) \end{bmatrix} = \begin{bmatrix} G_{11}(s) & G_{12}(s) \\ G_{21}(s) & G_{22}(s) \end{bmatrix} \begin{bmatrix} \hat{d}_1(s) \\ \hat{d}_2(s) \end{bmatrix} \quad (17)$$

where

$$G_{11}(s) = \frac{(sa_3 + 1)(s^2 b_2 + sb_1 + b_0)}{s(s^2 a_2 + sa_1 + a_0)} \quad (18)$$

$$G_{12}(s) = \frac{(sa_3 + 1)(s^2 c_2 + sc_1 + c_0)}{s(s^2 a_2 + sa_1 + a_0)} \quad (19)$$

$$G_{21}(s) = \frac{(sa_3 + 1)(s^2 e_2 + se_1 + e_0)}{s(s^2 d_2 + sd_1 + d_0)} \quad (20)$$

$$G_{22}(s) = \frac{(sa_3 + 1)(s^2 f_2 + sf_1 + f_0)}{s(s^2 d_2 + sd_1 + d_0)} \quad (21)$$

The values of  $a_0, a_1, a_2, a_3, b_0, b_1, b_2, c_0, c_1, c_2, d_0, d_1, d_2, e_0, e_1, e_2, f_0, f_1$  and  $f_2$  are defined by converter parameters and are presented in the appendix at the end of this paper.

It is clear, regarding (17) to (21), that the Double-Boost Converter constitutes a multivariable system, which can explain the physical behavior of the swing effect over the output voltages, because variations in duty cycle  $\hat{d}_1(s)$  acts over both outputs voltages  $\hat{V}_1(s)$  and  $\hat{V}_2(s)$  and conversely, variations in  $\hat{d}_2(s)$  implies also in changes in  $\hat{V}_1(s)$  and  $\hat{V}_2(s)$ , as can be represented by figure 7.

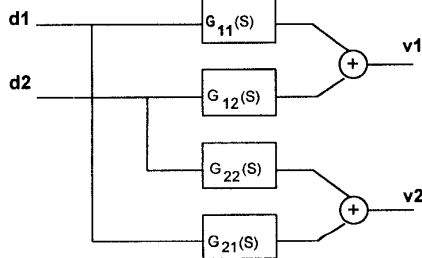


Figure 7: Double-Boost Converter Model

## 3 - CONTROL STRATEGY

The controller must have the capability to control, in an independent manner, the two PWM switches, in order to break the coupling between the output voltages and the duty cycles and to warrant the same conduction time for both switches, compensating by the signal drive, the intrinsic conduction time differences of these switches.

The control strategy is based upon the so-called Dynamic Uncoupling Technique, that provides a pre-compensation of the signals, performed by the inclusion of the inverse of the transference matrix already obtained, in the control loop, resulting in a diagonal transference matrix relating the output voltages and the duty cycles. With this technique voltage  $\hat{V}_1(s)$  will depend just of switch  $S_1$  duty cycle  $\hat{d}_1(s)$  and voltage  $\hat{V}_2(s)$  will depend just of switch  $S_2$  duty cycle  $\hat{d}_2(s)$ .

By applying this uncoupling technique it is possible, starting from one multivariable system, to reach a set of uncoupled monovariable systems (two systems in the present case).

In the resulting uncoupled systems, classic control techniques may be applied in order to control the two output voltages in an independent manner.

Figure 8 shows the Double Boost Converter and the pre-compensator.

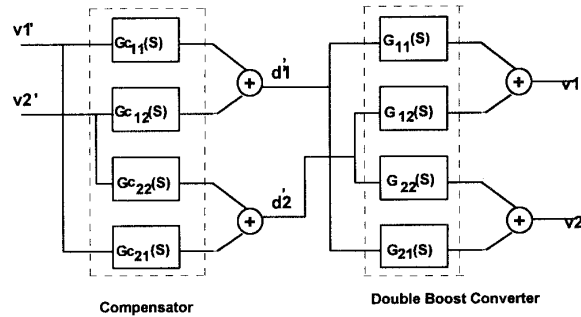


Figure 8: Double-Boost Converter and Compensator.

For Power Factor Correction applications, the signals  $\hat{d}_1(s)$  and  $\hat{d}_2(s)$  are used to generate the current reference for two UC3854 Integrated Circuits, which are responsible for the generation of the drive signals for the two PWM switches.

Figure 9 presents the basic scheme for Power Factor Correction (PFC), with average current control.

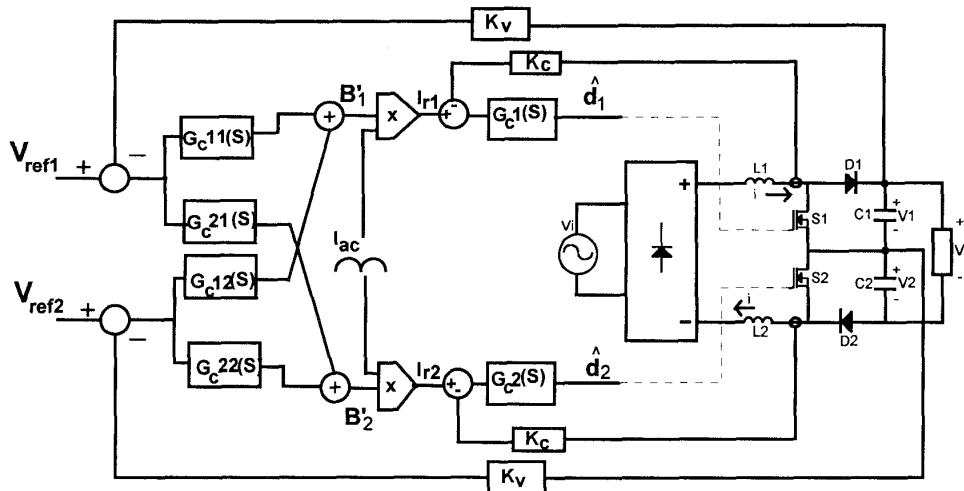


Figure 9: Basic scheme of PFC with average current control.

#### 4 - SIMULATIONS RESULTS

Numerical simulations were performed with the converter represented in figure 9, for the following basic specifications: Output Power:  $P_o=1600W$ ; Output Voltage:  $V_o=400V$ , Switching Frequency:  $f_s=70kHz$ ; Input Voltage:  $V_i=220 V_{rms}$ ; Line frequency:  $f_i=60 Hz$ .

Figure 10 shows the Double-Boost inductor current  $\hat{i}(s)$  and line voltage for one period. As may be seen, input current and line voltage are almost in-phase and high power factor is achieved, since the harmonic distortion of the input current is clearly small.

Figure 11 shows the output voltages  $V_1$  and  $V_2$  when voltage references  $V_{ref1}$  and  $V_{ref2}$  are set to equal values. As one can see, in this case the two output voltages present the same instantaneous values.

Figure 12 presents the output voltages  $V_1$  and  $V_2$  with voltage references  $V_{ref1}$  and  $V_{ref2}$  set to different values, in order to show the effect of independence of these two voltages. In fact it is possible to set these voltages to any value, even half of the output voltage  $V_o$  (this simulation was performed with 300 Hz to reduce time simulation). Figure 13 shows a detail of this output voltages.

Figure 14 shows the two control signals in the two UC3854 integrated circuits (employed to control independently the two PWM switches  $S_1$  and  $S_2$ ). For this case, the switch conduction and commutation

times are different, compelling the controls to establish different values for these signals.

Finally, Figure 15 shows the two UC3854 internal ramp signals related to the on-time duty cycles of the two main switches. Notice the control capability to change the slopes of the ramp signals.

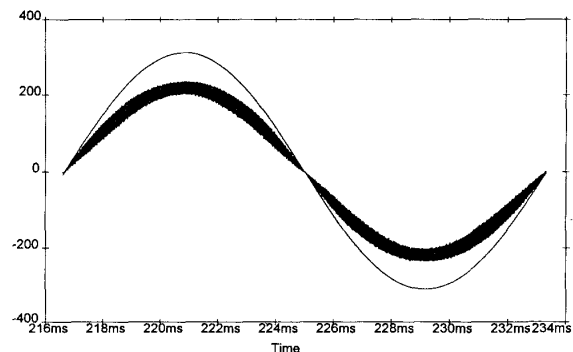


Figure 10: Inductor Current and line voltage (upper trace).

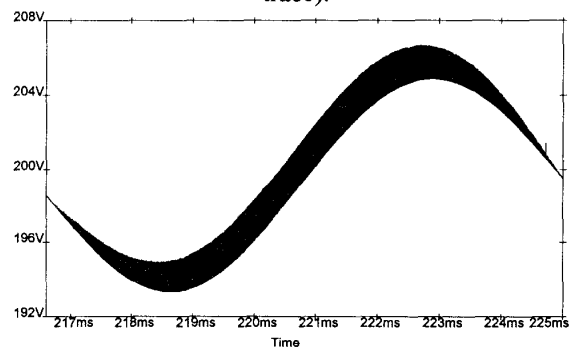


Figure 11: Output voltages  $V_1$  e  $V_2$  for normal operation (equal output capacitors voltages distribution)

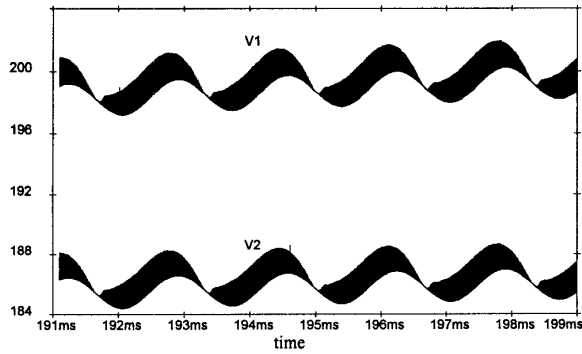


Figure 12: Output voltages  $V_1$  and  $V_2$  for two different references.

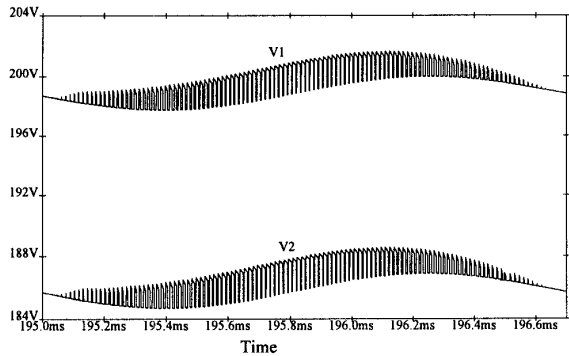


Figure 13: Detail of output voltages  $V_1$  and  $V_2$  for two different references.

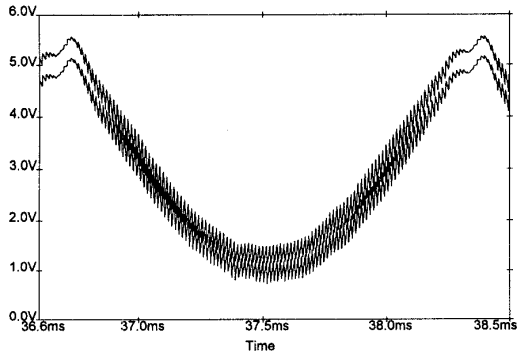


Figure 14: Control action for the two PWM switches

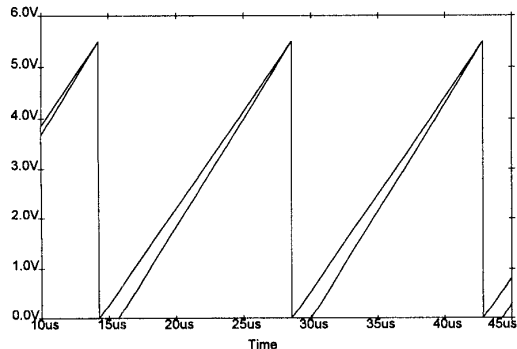


Figure 15: Two UC3854 internal ramp signal for the two main switches.

## 5 - CONCLUSION

In this paper a control strategy for the Double-Boost Converter for power factor correction application was proposed and analyzed. With the dynamic uncoupling technique it is possible to brake the coupling existing between the output voltages and the control variables, represented by the duty-cycle of the converter switches.

By transforming a multivariable system in a set of two monovaryable systems it is possible to apply classic control techniques to design the compensator for this particular converter.

Besides the modeling and analysis performed, results of numerical simulations were presented, to verify and validate the theoretical results obtained.

With this converter and with the control strategy proposed, high power factor for high power and a wide input voltage range variation can be achieved.

## 6 - REFERENCES

- [1] M. T. Zhang, Y. Jiang, F.C. Lee, "Single-Phase Three-Level Boost Power Factor Correction Converter", Proceedings APEC'95, pp.434-439.
- [2] D.Maksimovic, R.Erickson, "Universal-Input, High-Power-Factor, Boost Doubler Rectifiers", Proceedings APEC'95, pp 459-465.
- [3] Vorperian, V. , "Simplified Analysis of PWM Converters Using the Model of the PWM Switch", Seventh Annual Virginia Power Electronics Center Seminar - VPEC Seminar - Tutorials - Virginia/USA, 1989.

## APPENDIX

The coefficients of expressions (18) to (21) in section 2.2 are done by circuit parameters as presented by expressions (A.1) to (A.20).

$$a_0 = (C_1 + C_2)[DD'(r_{e1} + r_{e2}) + (R_{L1} + R_{L2}) + D^2 R] \quad (A.1)$$

$$a_1 = C_1 C_2 \{ (R + R_{se1} + R_{se2}) [(R_{L1} + R_{L2}) + DD'(r_{e1} + r_{e2})] + D^2 R (R_{se1} + R_{se2}) \} + (L_1 + L_2)(C_1 + C_2) \quad (A.2)$$

$$a_2 = C_1 C_2 (L_1 + L_2) (R + R_{se1} + R_{se2}) \quad (A.3)$$

$$a_3 = C_1 R_{se1} \quad (A.4)$$

$$b_0 = -I_L [(R_{L1} + R_{L2}) + DD'(r_{e1} + r_{e2}) + RD^2] \quad (A.5)$$

$$b_1 = -I_L \{ C_2 (R_{L1} + R_{L2}) (R + R_{se2}) + DD'C_2 [r_{e1} R_{se2} + r_{e2} (R_{se2} + R)] + D^2 C_2 R (r_{e1} + R_{se2}) + (L_1 + L_2) \} - V_1 R C_2 D' \quad (A.6)$$

$$b_2 = -I_L C_2 (L_1 + L_2) (R + R_{se2}) \quad (A.7)$$

$$c_0 = I_L [(R_{L1} + R_{L2}) + DD'(r_{e1} + r_{e2}) + RD'^2] \quad (A.8)$$

$$c_1 = I_L \{C_2 (R_{L1} + R_{L2}) R_{se2} + DD' C_2 [r_{e1} R_{se2} + r_{e2} (R_{se2} + R)] + D^2 C_2 R (-r_{e2} + R_{se2}) + (L_1 + L_2)\} + V_2 RC_2 D' \quad (A.9)$$

$$c_2 = I_L C_2 (L_1 + L_2) R_{se2} \quad (A.10)$$

$$d_0 = (C_1 + C_2) [DD'(r_{e1} + r_{e2}) + (R_{L1} + R_{L2}) + D'^2 R] \quad (A.11)$$

$$d_1 = C_1 C_2 \{(R + R_{se1} + R_{se2}) [(R_{L1} + R_{L2}) + DD'(r_{e1} + r_{e2})] + D'^2 R (R_{se1} + R_{se2})\} + (L_1 + L_2) (C_1 + C_2) \quad (A.12)$$

$$d_2 = C_1 C_2 (L_1 + L_2) (R + R_{se1} + R_{se2}) \quad (A.13)$$

$$d_3 = C_2 R_{se2} \quad (A.14)$$

$$e_0 = I_L [(R_{L1} + R_{L2}) + DD'(r_{e1} + r_{e2}) + RD'^2] \quad (A.15)$$

$$e_1 = I_L \{(R + R_{se1} + R_{se2}) [(R_{L1} + R_{L2}) + DD'(r_{e1} + r_{e2})] + D'^2 R (R_{se1} + R_{se2})\} + V_1 RC_1 D' \quad (A.16)$$

$$e_2 = I_L C_1 (L_1 + L_2) R_{se1} \quad (A.17)$$

$$f_0 = -I_L [(R_{L1} + R_{L2}) + DD'(r_{e1} + r_{e2}) + RD'^2] \quad (A.18)$$

$$f_1 = -I_L \{C_1 (R_{L1} + R_{L2}) (R + R_{se1}) + DD' C_1 [r_{e2} R_{se1} + r_{e1} (R_{se1} + R)] + D'^2 C_1 R (r_{e2} + R_{se1}) + (L_1 + L_2)\} - V_2 RC_1 D' \quad (A.19)$$

$$f_2 = -I_L C_1 (L_1 + L_2) (R + R_{se1}) \quad (A.20)$$

The parameters  $I_L$ ,  $V_1$ ,  $V_2$ ,  $D$  represent the DC operating point values for the boost inductor current,  $C_1$  capacitor voltage,  $C_2$  capacitor voltage and on-time duty cycle, respectively.